

QuickFF: A program for a quick and easy derivation of force fields for Metal-Organic Frameworks from ab initio input

L. Vanduyfhuys*, S. Vandenbrande*, T. Verstraelen*, R. Schmid†
M. Waroquier*, V. Van Speybroeck*

November 25, 2014

Email to: Veronique.VanSpeybroeck@Ugent.be

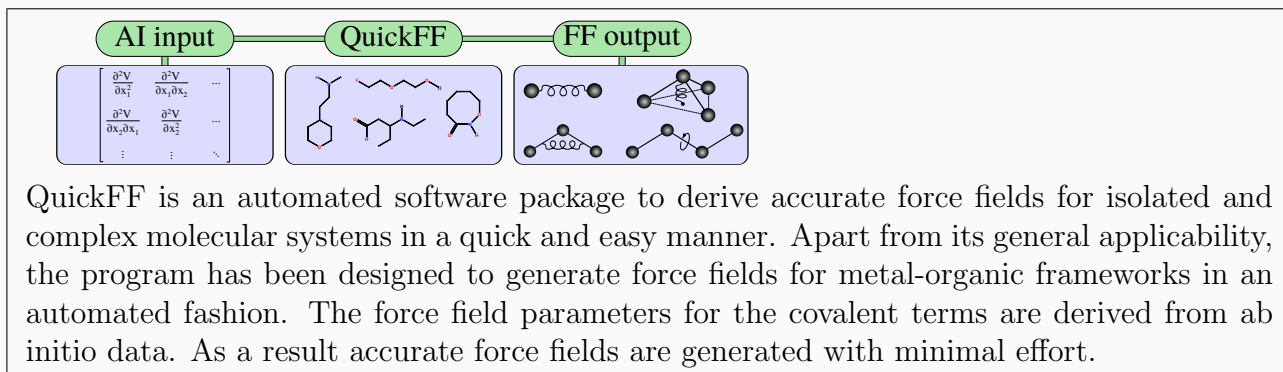
Abstract

QuickFF is an software package to derive accurate force fields for isolated and complex molecular systems in a quick and easy manner. Apart from its general applicability, the program has been designed to generate force fields for metal-organic frameworks in an automated fashion. The force field parameters for the covalent interaction are derived from ab initio data. The mathematical expression of the covalent energy is kept simple to ensure robustness and to avoid fitting deficiencies as much as possible. The user needs to produce an equilibrium structure and a Hessian matrix for one or more building units. Afterwards, a force field is generated for the system using a three-step method implemented in QuickFF. The first two steps of the methodology are designed to minimize correlations among the force field parameters. In the last step the parameters are refined by imposing the force field parameters to reproduce the ab initio Hessian matrix in Cartesian coordinate space as accurate as possible. The method is applied on a set of 1000 organic molecules to show the easiness of the software protocol. To illustrate its application to MOFs, QuickFF is used to determine force fields for MIL-53(Al) and MOF-5. For both materials accurate force fields were already generated in literature but they requested a lot of manual interventions. QuickFF is a tool that can easily be used by anyone with a basic knowledge of performing ab initio calculations. As a result accurate force fields are generated with minimal effort.

Keywords: QuickFF, automated software, force-field development, metal-organic frameworks, molecular simulation ■

*Center for Molecular Modeling (CMM), Ghent University, Technologiepark 903, 9052 Zwijnaarde, Belgium

†Lehrstuhl für Anorganische Chemie 2, Organometallics and Materials Chemistry, Ruhr-Universität Bochum, Universitätsstrasse 150, D-44780 Bochum, Germany



1 Introduction

Force fields have become a very powerful tool in molecular simulation nowadays. They are used in a very broad range of research fields to describe the inter- and intramolecular interactions of molecular systems. This is mainly because they allow to perform molecular simulations on a length and time scale inaccessible to ab initio calculations. The following examples show the versatility of their usage: the investigation of the protein-ligand structure for rational drug design¹⁻⁴, the design of new materials for methane storage⁵, the investigation of a molecular device for tetra-hertz signal processing⁶, the validation of continuum models describing the van der Waals interface in nanopumps⁷, the investigation of the ability of water in pure silica zeolites to absorb mechanical energy⁸, an atomistic study of the temperature influence on the reactivity of plasma species⁹, the investigation of adsorption of water and ions on carbon surfaces¹⁰. Specifically in the field of nanoporous materials and in particular metal-organic frameworks (MOFs), they are used intensively to study adsorption¹¹⁻¹³, diffusion^{11,14-16}, separation¹⁷ and breathing^{18,19} processes.

The literature on force field development is very rich and it is not possible to give a complete overview here. There are polarizable versus non-polarizable force fields, all-atom versus coarse-grained force fields, diagonal force fields versus force fields with cross terms, ... Another possible scheme to classify them can be the transferability, the range of systems to which they are applicable. On one hand, one has universal or general force fields, these are force fields that are applicable to a very wide range of systems, e.g. organic molecules. Examples of such force fields are UFF²⁰, GAFF²¹ and DREIDING²². Force fields like OPLS^{23,24}, AMBER²⁵⁻²⁷, CHARMM²⁸⁻³⁰, MM3³¹ and MM4³² can also be labeled as transferable, but between a more specific set of systems such as proteins or organic molecules. Recently various independent groups proposed automated procedures to derive force fields. The group of Barone developed JOYCE^{33,34}, a program to derive all-atom and united-atom force fields for small to medium-sized molecules. The force fields were parameterized by minimizing a cost function that measures the error between force field energy, gradient and Hessian on the one hand, and ab initio energy, gradient and Hessian on the other hand. However, the user

needs to determine weight factors for the different contributions in the cost function, which is a non-trivial task that has to be repeated for every molecule separately. These weight factors can be of crucial importance to get reliable results, especially for more complex systems¹⁸. The choice of these weight factors has a large impact on the correlations between rest values and force constants of harmonic force field terms. Another approach was used by the group of Ayers, they proposed an automated procedure for parameterizing Amber-compatible force fields³⁵. This procedure requires input from AMBER force fields and the force constants of the harmonic terms are derived by means of a term-by-term projection of the ab initio Hessian. Very recently, Huang and Roux proposed GAAMP³⁶, General Automated Atomic Model Parameterization, a program to derive AMBER or CHARMM compatible force fields. The harmonic terms were mainly taken from GAFF or CGenFF³⁷ and they focused their attention to the derivation of AMBER or CHARMM compatible charges and reliable potentials for soft dihedrals. Mayne et al. developed the Force Field Toolkit as a VMD plug-in to automatically parametrize CHARMM compatible force fields for small molecules³⁸. Also very recently, Stefan Grimme developed QMDFE (Quantum Mechanically derived Force Field)³⁹, a procedure to automatically derive force fields from quantum mechanical input. The methodology also includes a parameterization of the van der Waals interactions inspired by earlier work of Grimme regarding DFT-D3⁴⁰. The FF was shown to be accurate for organic molecules and transition metal complexes. However, the rest values of the covalent terms are systematically set to the ab initio equilibrium values. It remains to be tested whether this remains valid for MOFs, especially if a force field is used with no exclusions of 1-2 and 1-3 electrostatic interactions.

The development of a new program package QuickFF for deriving force fields, is inspired by the general quest from the MOF-community to develop in a transparent way accurate force fields for these systems. New MOFs are being synthesized at a considerable rate. Furthermore, large databases of hypothetical MOFs have been proposed^{41,42} recently. A tool that is able to generate force fields with a minimum of manual interventions would be very valuable to screen a large number of materials in a fast and easy way. Once force fields are generated they may be used in molecular dynamics (MD) and Monte-Carlo (MC) sim-

ulations to describe phenomena, with a fixed connectivity of the material, not reachable by quantum mechanical approaches due to the high computational cost. MOFs differ from other nanoporous materials, such as zeolites, in various aspects, but the specific framework flexibility is by far the feature that attracts the most attention. This lattice flexibility has a strong influence on physical properties such as elastic constants, thermal conductivity, diffusion^{14,43} and adsorption properties of guest molecules in the pores⁴⁴⁻⁴⁸. The latter phenomenon is mostly referred to as the breathing effect⁴⁹⁻⁵¹, by which the host framework can shrink or expand. The force fields generated by QuickFF need to be able to describe these processes, which is a very challenging task.

When generating force fields for MOFs, special attention needs to be paid to describe the metal-ligand bond. Indeed these interactions are not easily described by suitable coordination bond terms in force fields, as they may also have large ionic contributions. For the organic linker a wealth of reliable FFs exists in literature but the combination of organic entities with inorganic building blocks poses extra complexities. Recently various groups have proposed theoretical schemes to construct force fields for MOFs. First of all MOF-FF was developed by the group of Schmid et al. The force field energy expression is very similar to the MM3 expression³¹ and includes cross terms and anharmonic bonds.⁵²⁻⁵⁴ The electrostatic interactions are described using Gaussian charges. The covalent parameters are fitted to ab initio cluster data using a genetic algorithm. MOF-FF has been able to produce accurate force fields for a series of well known MOFs such as MOF-5, HKUST-1, UIO-66 and others. During the fitting procedure of the force fields, additional user interference could be necessary to adjust the allowed range of the parameters or to run several parallel genetic algorithm runs and to combine them afterwards.⁵⁵

Very recently the group of Walsh et al. developed the BTW-FF procedure⁵⁶. Periodic ab initio calculations are used to fit the force field. The energy expression is identical to that of the MM3 force field. Some initial parameters have been refined from existing force fields (MM3 and MOF-FF). The reparameterization of the MM3 force field includes the terms describing the carboxylic head and interaction between metal node and ligand. New

parameters were also derived for the metal node, particularly for the metal-inorganic oxygen interactions. Charges are derived from the periodic wave function using Bader analysis⁵⁷. The resulting force fields have been used to calculate bulk moduli, thermal expansion coefficients and heat capacities. Presently, BTW-FF has been parameterized for a set of well known MOFs such as MOF-5, HKUST-1, UiO-66 and others. Finally UFF4MOF⁵⁸ is an extension for the well-known Universal Force Field to describe metal-organic frameworks. New parameters are provided for Al and all row four transition metal elements. Furthermore, additional O parameters are proposed that provide reliable structures of the metal oxide clusters of the connectors. These extra parameters were extracted from fits to ab initio cluster calculations. This extension can be used to construct a UFF force field for any MOF containing row 4 transition metals or Al. Although UFF4MOF has been shown to be very accurate in reproducing the unit cell dimensions of several MOFs, it needs to be tested in how far the parameter set will be accurate enough to simulate more exotic MOFs or physical phenomena that are more sensitive to the specific shape of the potential energy surface, such as breathing.

QuickFF is an easy to use program that uses as input the equilibrium geometry and the Hessian matrix elements in cartesian coordinates. The intention is to derive force fields based on a maximal transfer of knowledge from the quantum mechanical system and that are transferable to larger systems. We implemented the procedure in a user-friendly Python code. Currently, the Python code is written to read formatted checkpoint files of a frequency job performed in Gaussian⁵⁹, but it can easily be extended to read input from other programs.

The paper is structured as follows. In section 2 we briefly discuss the methodology as embedded in QuickFF for the derivation of force fields from ab initio calculations and elaborate on the practical usage. In section 3.1 the method is applied on a set of 1000 organic molecules to illustrate the ease with which one can derive accurate force fields for a large test set. As a proof of principle for the construction of force fields on MOFs, QuickFF is used to construct a force field for Mil-53(Al) and for MOF-5 (section 3.2).

2 Implemented methods for generation of force fields with QuickFF

2.1 Force field potential energy expression

In a force field, the various contributions to the potential energy are expressed in terms of atom types, i.e. atoms with a similar chemical identity. In QuickFF, the atom type of each atom can be determined automatically based on local environment, or defined manually by the user. More information about the automatic assignation of atom types can be found in the Supporting Information. The force fields generated with QuickFF are composed of three contributions: a valence contribution describing covalent interactions between chemically bonded atoms ($V_{\text{cov}}^{\text{ff}}$), a van der Waals part describing the Pauli repulsion and dispersion interactions (using a Lennard-Jones or an MM3-Buckingham potential) and an electrostatic contribution governed by the Coulomb interaction between point charges or Gaussian distributed charge densities ($V_{\text{el}}^{\text{ff}}$):

$$V^{\text{ff}} = V_{\text{cov}}^{\text{ff}} + V_{\text{vdW}}^{\text{ff}} + V_{\text{el}}^{\text{ff}} \quad (2.1)$$

$$V_{\text{vdW}}^{\text{ff}} = \begin{cases} \frac{1}{2} \sum_{\substack{i,j=1 \\ (i \neq j)}}^{N_{\text{at}}} \epsilon_{ij} \left[1.84 \cdot 10^5 \cdot e^{-12 \frac{r_{ij}}{\sigma_{ij}}} - 2.25 \left(\frac{\sigma_{ij}}{r_{ij}} \right)^6 \right] & \text{(MM3)} \\ \frac{1}{2} \sum_{\substack{i,j=1 \\ (i \neq j)}}^{N_{\text{at}}} 4\epsilon_{ij} \left[\left(\frac{\sigma_{ij}}{r_{ij}} \right)^{12} - \left(\frac{\sigma_{ij}}{r_{ij}} \right)^6 \right] & \text{(LJ)} \end{cases} \quad (2.2)$$

$$V_{\text{el}}^{\text{ff}} = \frac{1}{2} \sum_{\substack{i,j=1 \\ (i \neq j)}}^{N_{\text{at}}} \frac{Q_i Q_j}{4\pi\epsilon_0 r_{ij}} f(r_{ij}) \quad (2.3)$$

with

$$f(r_{ij}) = \begin{cases} 1 & \text{point charges} \\ \text{erf} \left(\frac{r_{ij}}{d_{ij}} \right) & \text{Gaussian charges} \end{cases} \quad (2.4)$$

N_{at} is the total number of atoms in the system, Q_i is the charge of atom i and r_{ij} is the distance between atoms i and j , erf is the error function and $d_{ij} = \sqrt{d_i^2 + d_j^2}$ is the mixed radius of the Gaussian charges (d_i is the radius of the Gaussian charge distribution of atom i).

The valence contribution to the potential energy has the following mathematical form:

$$V_{\text{cov}}^{\text{ff}} = V_{\text{bond}} + V_{\text{bend}} + V_{\text{torsion}} + V_{\text{oopdist}} \quad (2.5)$$

$$V_{\text{bond}} = \sum_{i=1}^{N_r} \frac{1}{2} K_{r,i} (r_i - r_{0,i})^2 \quad (2.6)$$

$$V_{\text{bend}} = \sum_{j=1}^{N_\theta} \frac{1}{2} K_{\theta,j} (\theta_j - \theta_{0,j})^2 \quad (2.7)$$

$$V_{\text{torsion}} = \sum_{k=1}^{N_\phi} \frac{1}{2} K_{\phi,k} [1 - \cos(m_k (\phi_k - \phi_{0,k}))] \quad (2.8)$$

$$V_{\text{oopdist}} = \sum_{l=1}^{N_d} \frac{1}{2} K_{d,l} (d_l - d_{0,l})^2 \quad (2.9)$$

The force field includes harmonic bonds V_{bond} , harmonic bends V_{bend} , cosine dihedrals V_{torsion} and harmonic out-of-plane distances V_{oopdist} . N_r is the total number of stretch bonds, N_θ the number of bending angles, N_ϕ the number of dihedral angles, and N_d the number of out-of-plane distances. An out-of-plane distance represents the distance from a plane determined by 3 atoms to a fourth atom that is only bonded to each of these 3 atoms (see figure 1). These out-of-plane distances are related to out-of-plane bends⁶⁰, also called inversion terms. We prefer to work with out-of-plane distances because for every out-of-plane pattern, there is a unique out-of-plane distance. The introduction of out-of-plane terms enables us to accurately describe both the planarity of conjugated π -systems and the non-planarity of some sp^3 -units such as amines. The valence FF contains several unknown parameters: force

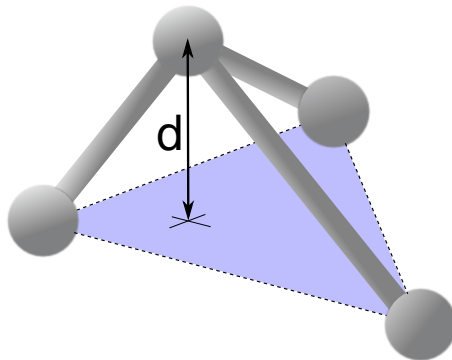


Figure 1: Illustration of the out-of-plane distance d

constants ($K_{r,i}$, $K_{\theta,j}$, $K_{\phi,k}$ and $K_{d,l}$), rest values ($r_{0,i}$, $\theta_{0,j}$, $\phi_{0,k}$ and $d_{0,l}$) and multiplicity

factors (m_k). All these parameters will be estimated in such a way that the force field reproduces the ab initio equilibrium geometry and ab initio Hessian in equilibrium as well as possible.

To account for the van der Waals (vdW) interaction, a repulsive short-range term—modeling the Pauli exclusion principle—and attractive long-range dispersion terms should be added to the force field potential. In the current version of QuickFF two vdW potentials are implemented, the Buckingham potential, as used in MM3³¹, and the Lennard-Jones (LJ) 6-12 type potential, as used in UFF²⁰. The repulsive interaction is described better by the exponential part of the Buckingham potential than by the steep r^{-12} part of the LJ potential. The user has the choice to use one of the implemented potentials. More details on the practical implementation of these van der Waals interactions can be found in section 2.3. If necessary, QuickFF can easily be extended with other van der Waals schemes such as the ones developed by Grimme and coworkers.

The last contribution to the FF potential is the electrostatic interaction. Atomic point charges can be derived from the quantum mechanical wave function belonging to the equilibrium geometry using one of the various partitioning schemes available in literature, e.g. Hirshfeld-I^{61,62}, Hirshfeld-E⁶³, RESP⁶⁴ charges, ... Hirshfeld based schemes apply the atom-in-molecule (AIM) principle to partition the ab initio molecular electron density into overlapping atomic electron densities from which the charges can be derived. The RESP method estimates point charges by fitting them to the ab initio electrostatic potential. In QuickFF the user is free to apply one of the available charge population schemes. The derivation of atomic charges is not part of the QuickFF procedure. Only the exclusion rule for the non-bonding interactions should still be chosen. An option is built in to exclude some interatomic electrostatic force terms (for example 1-3, 1-4 bonded pairs). More details on the practical implementation of these electrostatic interactions can be found in section 2.3.

2.2 Parameterization protocol implemented in QuickFF

The parameterization implemented in QuickFF aims at determining values for the force constants and rest values figuring in the covalent part of the force field expression. A small note regarding the nomenclature is in order. In this work, the term rest value is used for the parameters figuring in the harmonic energy term expressions, while the term equilibrium value is used for the value of an internal coordinate in the equilibrium structure. These two values are not necessarily identical (which is also illustrated in the Supporting Information), as opposed to many force fields. The procedure consists of three steps as explained below.

2.2.1 Step 1 - Determining the dihedral multiplicities and rest angles

In the first step the dihedral multiplicities m_k and rest angles $\phi_{0,k}$ are determined directly from the equilibrium geometry based on local symmetry. Dihedral patterns belonging to the same atom types may have widely varying equilibrium angles. For example, the H-C-C-H dihedrals in ethane have values of 60, 180 and 300 degrees. Hence, the dihedral potential should have local minima at each of these values. Therefore, we need to choose the multiplicity and rest angle accordingly, which is $m_k = 3$ and $\phi_{0,k} = 60^\circ$ in the case of ethane. The general procedure for determining m_k and $\phi_{0,k}$ is explained in detail in the Supporting Information. In some cases this procedure will not result in a unique dihedral potential of the type as given in expression (2.8) because of its simple mathematical form; we then choose to ignore that dihedral all together, in accordance with the QuickFF philosophy. If necessary one could construct more complicated forms of the potential afterwards to represent the dihedral angles in particular cases, such as internal rotors^{36,39,65}.

2.2.2 Step 2 - perturbation trajectories

In a second step a new methodology is implemented to determine values of the force constants and rest values and addresses the correlation between the force field parameters. To this end trajectories are constructed along the multidimensional potential energy surface (PES)

near the equilibrium structure. Changes to the potential energy along such trajectories can be modeled with the suggested FF expressions and compared with the first principles predictions, achieved by a second order Taylor expansion of the ab initio PES along the perturbation trajectory. Force field parameters can be extracted directly from the ab initio Hessian for each IC consequently by carefully choosing the trajectories. This is an important feature, as it doesn't require an ambiguous Cartesian-to-IC transformation of the Hessian, nor does it require complicated cost functions. As a result, a unique set of force field parameters will be obtained. In this section, we will briefly outline this procedure, more details can be found in the Supporting Information. To extract the force field parameters for a certain IC, we construct so-called perturbation trajectories. Each frame in the trajectory corresponds to a certain perturbation imposed on the IC under consideration. Consider a particular IC q_n and assume some small perturbation bringing it to the value \tilde{q}_n . The geometry corresponding to this perturbation is determined by relaxing all other degrees of freedom (apart from q_n) by minimizing the strain corresponding to all these other degrees of freedom. The strain is quantified by means of the following function:

$$\chi_n^S(\vec{R}) = \frac{1}{2} \sum_{m \neq n} \left[q_m(\vec{R}) - q_m(\vec{R}_0) \right]^2 \quad (2.10)$$

The summation runs over all internal coordinates q_m , different from the perturbed IC q_n . Each IC in the summation is expressed in atomic units as a means of preconditioning. Repeating this procedure of minimal internal strain for several perturbation values \tilde{q}_n ¹ yields trajectories $\vec{R}(\tilde{q}_n)$ along an internal coordinate q_n , that are as much as possible decoupled from the other IC's and in which all other IC's are relaxed as much as possible. Hence, all contributions to the covalent force field energy along the trajectory will be small, except for the harmonic term related to q_n . Therefore, we approximate the covalent force field energy $V_{\text{cov}}^{\text{ff}}(\tilde{q}_n)$ along the perturbation trajectory, by a single harmonic potential in \tilde{q}_n .

$$V_{\text{cov}}^{\text{ff}}(\tilde{q}_n) = \frac{K_n}{2} (\tilde{q}_n - q_{n,0})^2 \quad (2.11)$$

instead of the full expression of the covalent energy, where the variations of all bond lengths, bending angles, out-of-plane distances and dihedral angles are taken into account. The

¹By default the procedure is repeated for 11 frames, with perturbations in a range of 0.05 Å for distances and 5 ° for angles.

unknown force field parameters figuring in expression 2.11, i.e. K_n and $q_{n,0}$, can now be estimated by expressing that the force field energy should be equal to the ab initio energy along the perturbation trajectory, apart from a constant shift c , for each chosen \tilde{q}_n :

$$V^{\text{ai}}(\vec{R}(\tilde{q}_n)) = V_{\text{el}}^{\text{ff}}(\vec{R}(\tilde{q}_n)) + V_{\text{vdW}}^{\text{ff}}(\vec{R}(\tilde{q}_n)) + \frac{K_n}{2}(\tilde{q}_n - q_{n,0})^2 + c \quad (2.12)$$

Hence, one can fit a parabola to the difference between V^{ai} and $V_{\text{el}}^{\text{ff}} + V_{\text{vdW}}^{\text{ff}}$ yielding directly an estimate of the force constant K_n and rest value $q_{n,0}$. The procedure can be repeated for each internal coordinate q_n , however, we only apply it to bond lengths, bending angles and out-of-plane distances. No dihedral angles are considered in this step of the procedure. The main reason is that the goal of this step is to get accurate estimates of the rest values, while the rest values of the dihedral angles were already determined in the previous step based on local symmetry. Finally, an averaging procedure is applied to all IC's belonging to the same atom types. The standard deviation can be regarded as a measure to assess the quality of the atom types which compose the IC's.

The force constants derived in this step are overestimated because even along the perturbation trajectories with minimal strain, coupled IC's cannot be completely decoupled and that by consequence contributions from other IC's along the trajectory $\vec{R}(\tilde{q}_n)$ should be considered instead of the single harmonic potential of Eq. (2.11). The third step consists of a fine tuning to address this error and match the force field Hessian with the ab initio Hessian.

2.2.3 Step 3 - refinement of the force constants

In the third step, the harmonic force constants from the previous step are refined, and the still missing dihedral force constants are fitted according to a simple least-square cost function that measures the error between the various ab initio Hessian and the force field Hessian matrix elements expressed in Cartesian coordinates:

$$\chi^H(\vec{K}) = \sum_{i \leq j} \left([\mathbf{H}^{\text{ai}}]_{ij} - \frac{\partial^2 V_{\text{el}}^{\text{ff}}}{\partial R_i \partial R_j} - \frac{\partial^2 V_{\text{vdW}}^{\text{ff}}}{\partial R_i \partial R_j} - \frac{\partial^2 V_{\text{cov}}^{\text{ff}}}{\partial R_i \partial R_j}(\vec{K}) \right)^2 \quad (2.13)$$

\vec{K} represents a vector containing all force constants. All force constants are constrained to be positive. In addition, we impose that all dihedral force constants are smaller than 200 kJ/mol to prevent possible compensation effects. The rest values, as extracted from step 2,

are kept fixed. In this way, troublesome fitting deficiencies due to the correlations between force constants and rest values are avoided. The constrained optimization is performed using the Sequential Least Squares Programming⁶⁶ algorithm.

2.3 Practical usage

QuickFF can be used in two ways: from a command-based terminal by means of a single command using the script `qff-est.py` or by writing an external script and importing QuickFF as a Python library. The former is very straightforward to use and will be outlined in this section, the latter is less straightforward but allows more control. Both usages are also documented on line at <http://molmod.github.io/QuickFF/>.

The most straightforward way to construct a force field from the command line is by means of the following command:

```
qff-est.py [options] fns
```

`fns` is a space-separated list of input file names, while `options` is a list of space-separated optional keyword arguments with the format `--key=value`. Several input file formats are supported for reading input data. For example, a Gaussian formatted checkpoint file can be specified to read the ab initio geometry, forces and Hessian in equilibrium and a HDF5 file can be used to specify the electrostatic and/or van der Waals parameters. All supported file formats are discussed in detail in the on-line documentation. The optional keyword arguments can be used to control the force field model, all of these options are documented on line as well as by means of the `--help` option. The list below enumerates the most important options:

- `--atypes-level`: the level of automatic atom type assignation (`low`, `medium`, `high` or `highest`) as explained in the Supporting Information. By default, the atom types are taken from the input files.
- `--ei-model`: Defines the potential used for the electrostatic interactions. Can be `CoulPoint`, `CoulGauss`, `HarmPoint`, `HarmGauss` or `Zero`. The Harm variants use a second order Taylor expression to speed up the calculation considerably (and remain accurate). The default is `HarmPoint`.

- `--ei-scales`: Defines the scaling rule for the electrostatic interactions. Three comma-separated floats are required. The first one sets the scale for atoms separated by 1 bond, the second for atoms separated by 2 bonds and the third for atoms separated by 3 bonds. The default is `0.0,0.0,1.0`.
- `--ei-path`: Defines the path in the HDF5 file, given as an input file, from which the charges (and optionally the radii in case gaussian distributed charges are required) will be extracted.
- `--vdw-model`: Defines the potential used for the van der Waals interactions. Can be `LJ`, `MM3`, `HarmLJ`, `HarmMM3` or `Zero`. The default is `Zero`.
- `--vdw-scales`: Defines the scaling rule for the van der Waals interactions. Three comma-separated floats are required. The default is `0.0,0.0,1.0`.
- `--vdw-path`: Defines the path in the HDF5 file, given as an input file, from which the van der Waals parameters, epsilons and sigmas, will be extracted.

To illustrate the usage of the `qff-est.py` script, suppose one disposes of a Gaussian formatted checkpoint file (`gaussian.fchk`) that is the result of a frequency job performed on the equilibrium geometry and a HDF5 file (`gaussian.wpart.h5`) that contains Iterative Hirshfeld charges in the path `/wpart/hi`. One can now easily construct a force field using automatically assigned atom types according to the level `high`, containing a covalent term for all IC's, an electrostatic part in which all atom pairs are allowed to interact (including bonded atoms) using the Iterative Hirshfeld point charges and no van der Waals terms. This can be achieved by means of the following command:

```
qff-est.py --atypes-level=high --ei-path=/wpart/hi --ei-scales=1,1,1
gaussian.fchk gaussian.wpart.h5
```

The option `--ei-model` is not needed here because its default value is the desired one.

3 Applications

3.1 QuickFF on a large set of organic molecules

The ease of generating accurate force fields in a fast and efficient way for a large set of molecules is illustrated by applying the program on a set of 1100 organic molecules. To this end, 1100 molecules were randomly selected from a subset of the PubChem Compound database⁶⁷. Several selection criteria were introduced to define a subset that can be accepted as sufficient for a serious assessment of the QuickFF procedure for deriving force fields. The detailed procedure to select randomly a thousand molecules from an initial set of 408366 molecules from the PubChem Compound database is outlined in the Supporting Information (SI). To illustrate the chemical diversity in this final set of molecules, we constructed various histograms, shown in Figure 2. The figure illustrates the distribution of several properties: the total number of atoms in a molecule, the number of C, H, N and O atoms in a molecule, the size of cyclic patterns and the hybridization of C, N and O atoms. OpenBabel⁶⁸ was used to determine the hybridization of each atom.

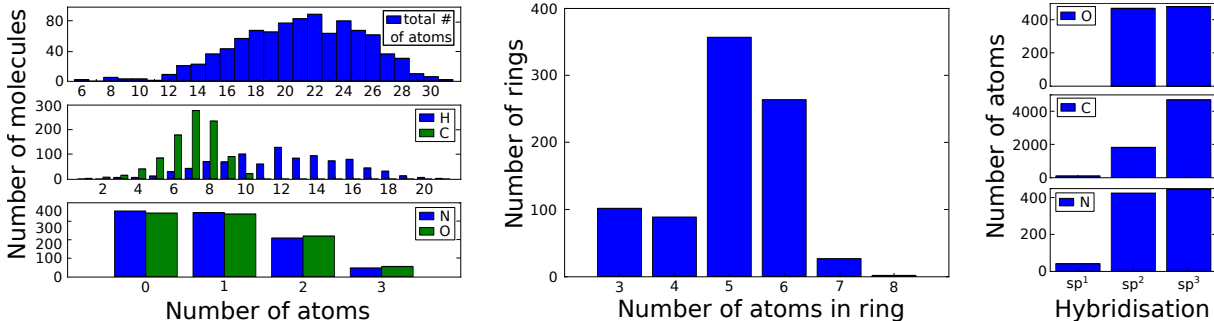


Figure 2: Histograms to illustrate the diversity of the test set. Left: distribution of the total number of atoms in a molecule and number of C, H, O and N atoms in a molecule. Middle: distribution of the size of cyclic patterns. Right: distribution of the hybridization of C, N and O atoms.

For every molecule in this set, ab initio calculations have been performed to generate the reference data, serving as input for the derivation of the force field. First, the geometry of the molecule was optimized and the ab initio Hessian was constructed with corresponding frequencies using Density Functional Theory (DFT). The B3LYP⁶⁹⁻⁷¹ density functional was

chosen for its well-known accuracy in describing small molecules consisting of first and second row atoms^{72,73}, together with the 6-311+G(d,p) basis set⁷⁴⁻⁷⁶. These calculations were performed with the Gaussian 09⁵⁹ program. The optimization was done using the VeryTight convergence criterion and the SCF(tight,xqc) and int(grid=ultrafine) options were selected for both the optimization and frequency tasks. Next, the atomic charges were computed using the Hirshfeld-E⁶³ partitioning scheme with Horton⁷⁷, a development platform for electronic structure methods. With the Gaussian output and the atomic charges, we derived a force field using QuickFF without an electrostatic exclusion rule, and atom types derived according to the atom type level ‘high’ (see Supporting Information). Next, the force fields were used to perform a geometry optimization and to calculate the Hessian with YAFF⁷⁸, an in-house developed force-field code for molecular simulations of both periodic and non-periodic systems. Finally, the frequencies were calculated using TAMkin⁷⁹, a post-processing toolkit for normal mode analysis, thermochemistry and reaction kinetics. One remark concerns the ab initio method used to generate the reference data. Due to computational efficiency DFT methods are mostly preferred. For the training set used here B3LYP was selected, which includes no dispersion interaction. In this case the van der Waals interactions can be added to full strength afterwards to the force field potential without the risk of double counting, as the reference ab initio data did not contain any dispersion forces. For some molecules accurate geometries may only be obtained by using functionals including long-range dispersion (such as M06-2X^{80,81}) or with B3LYP+D3 correction terms of Grimme⁴⁰ (at each optimization cycle). Fitting the parameters of the bonded FF terms indirectly incorporates the influence of dispersion. Including additional vdW terms to the total FF potential may lead to an overestimation of the dispersion effects. One can account for this double counting by introducing a scale factor to the non-bonded interactions, but there is no conclusive protocol to fix it. Another possibility is to restrict the vdW terms to 1,4 interactions and higher, i.e. excluding 1,2 and 1,3 interactions, to restrict the van der Waals terms from influencing the bond lengths and bending angles

The quality of the force fields generated by QuickFF for the large data set is first validated by comparing equilibrium bond lengths, bending angles, dihedral angles, out-of-plane distances and frequencies with regard to the reference data and by comparing its perfor-

mance to the results obtained with two well-known general force fields, UFF²⁰ and GAFF²¹. These two force fields are universal force fields adjusted to reproduce mostly experimental data. The validity of QuickFF on small organic units is also a necessary condition for its application to hybrid materials such as MOFs.

The results are shown in Figure 3 for four force fields (QuickFF with van der Waals terms taken from UFF, QuickFF without van der Waals terms, GAFF and UFF). Each row in Figure 3 displays the scatter plots of a certain observable (bond lengths, bending angles, ...). Each dot represents the value of an internal coordinate or a vibrational mode of a molecule in the data set. The x-value represents the ab initio value, while the value on the y-axis reports the force field prediction. The diagonal line corresponds to the situation where the force field exactly reproduces the ab initio reference value. Above each scatter plot, the standard deviation is included, which gives an indication of the error between the force field predictions and the ab initio reference data.

The scatter plots of Figure 3 show that QuickFF performs very well compared to the other general force fields. The standard deviation of any observable is lower for QuickFF than for both GAFF and UFF (except for the dihedrals, see later). This is not really surprising since the QuickFF parameters have been fitted for each molecule separately and sufficient flexibility was taken into account in the assignment of atom types. By construction the two universal FF's GAFF and UFF allow less flexibility in the assignment of atom types. Bond lengths are relatively well reproduced but a significantly larger scattering is noticed for the bending angles. The lack of an out-of-plane (oop) term in the covalent force field expression in GAFF and UFF gives rise to a cross pattern centered at the origin. It implies that ab initio and force field predictions for the out-of-plane structure belonging to the equilibrium geometry are not consistent with each other. Planar configurations may result from ab initio calculations, while force fields rather predict a non-planar equilibrium, or vice versa. In the scatter plots, these cases give rise to the presence of horizontal and vertical branches. No such cross pattern is present in the scatter plot of QuickFF, which clearly illustrates the added value of the valence force field terms containing the oop distances.

The series of scatter plots related to the dihedral angles show that these internal degrees of freedom are more difficult to reproduce with all investigated force fields. This could

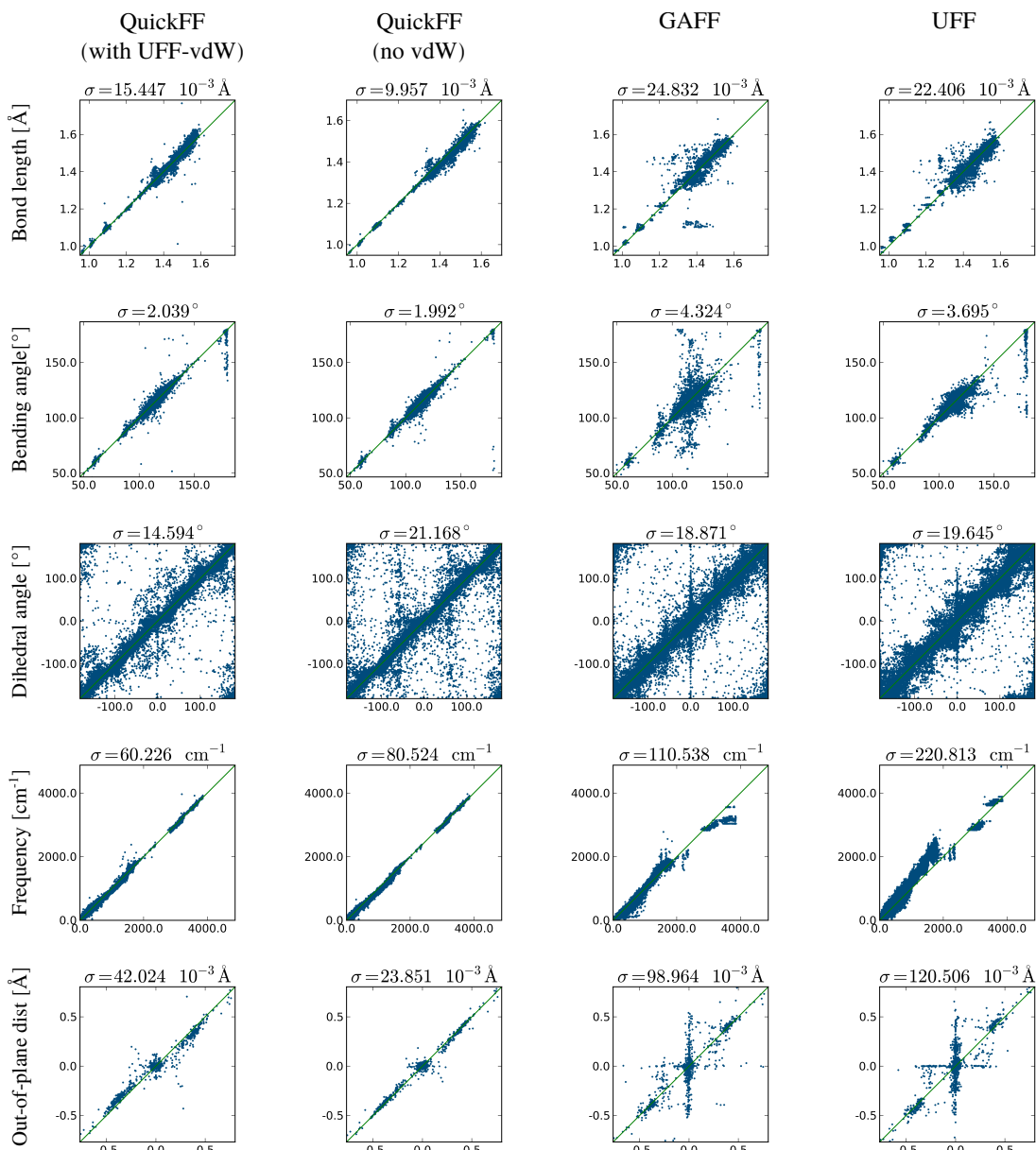


Figure 3: Scatter plots visualizing the performance of the force fields (QuickFF (with vdW from UFF), QuickFF (without vdW), GAFF and UFF) in reproducing geometrical quantities and frequencies with respect to the ab initio reference data. The x-value reports the ab initio value of the various properties for each molecule of the data set, while the FF prediction is given on the y-axis.

be anticipated because soft dihedral angles, e.g. dihedrals related to internal rotors, are typically the internal degrees of freedom that are the most flexible. Moreover, these soft

dihedrals correspond to anharmonic motions while the Hessian used in the reference data for QuickFF only involves harmonic motions. Hence, insufficient information is incorporated in the model to accurately fit the force field terms of soft dihedrals. As QuickFF is designed to accurately generate first-generation force fields for a large set of molecules, this does not pose a serious problem. In cases where such soft dihedral angles come into play prominently, a second generation force field can be built including information on the torsional potential of the internal rotor. Such refinements come at a higher computational cost as additional ab initio data need to be performed, as such this procedure is not taken up in the standard workflow of QuickFF which is designed to generate force fields in a fast and easy way.

The scatter plots of Figure 3 further reveal that van der Waals interactions only have a small impact on the geometry and the frequencies of these small organic molecules. However, one must be careful not to extrapolate these conclusions to larger molecules without further investigation. As our final aim is the construction of a transparent methodology for hybrid materials, these extensions are beyond the scope of the present article.

3.2 Quick and easy force field generation for MIL-53(Al) and MOF-5

The main reason to develop QuickFF is to have a transparent and easy protocol for the construction of viable force fields for metal-organic frameworks. Easy generation of force fields for these materials could be beneficial to screen these materials quickly for optimal properties. Hereafter QuickFF is used to generate force fields for two materials MIL-53(Al)⁸² and MOF-5⁸³. MIL-53(Al) was chosen as it is one of the prototype MOFs that shows an intriguing flexible behavior, having the capacity to undergo large structural deformations. For this material, some of the present authors already constructed a force field earlier, but the procedure required various manual interventions and can not be regarded as quickly applicable to a larger set of materials¹⁸. However the original constructed force field was very accurate, as it was able to reproduce the breathing behavior of the material properly and predict the transition pressure of the mechanically induced transition from large pore to narrow pore⁸⁴. QuickFF can only be approved for further applications if it equally well reproduces all these properties. The other benchmark system is MOF-5, which is the first MOF for which a specific force field was developed by the group of Schmid et al.⁵² This force

field was able to reproduce geometry, negative thermal expansion and benzene diffusion.

3.2.1 Validation for MIL-53(AI)

The generation of the force field for MIL-53(AI) relies on ab initio calculations on two isolated clusters, which are representative for the metal-oxide unit at one hand and the terephthalate linker on the other hand (see Figure 4). The computational details can be found in ref. 18. In a next step, QuickFF is applied to each individual clusters. To be consistent with our previous work, some assumptions are made, which facilitates the comparison of the newly derived QuickFF force field directly with our previous force field. First, no van der Waals interactions were included a priori, instead they will be added a posteriori and taken from the MM3 force field. Second, we include all electrostatic interactions without any exclusions and we use the same charges. Third, a covalent term was associated with all internal coordinates. As out-of-plane vibrations have not been included in the covalent terms of the previous FF, we constructed two force fields with QuickFF with and without $V_{oopdist}$. As a result the performance of the two force fields can be compared on equal basis, and at the same time the added value of the out-of-plane term in the covalent interaction can be examined.

In a next step, the data of the individual clusters need to be merged to produce a force field for the periodic crystal. The same procedure was followed as in our earlier work, in which a core region is defined in both systems. These core regions are illustrated in Figure 4 and consist of atom types that are considered relevant for the periodic crystal. From each cluster force field, energy terms are only retained when their internal coordinates have at least one atom in the core region. Whenever a term is present in the force fields of both clusters, their parameters are averaged over both clusters. The resulting force field parameters can be found and compared with our previous force field in the Supporting Information. This comparison reveals that the force field parameters are not differing much from each other, the largest deviations are noticed in the dihedrals. The concept applied here nicely illustrates how to build force fields for periodic systems from ab initio data generated on smaller building units. Such a procedure is beneficial in terms of computational time, as the computation of accurate Hessians for periodic systems is non-trivial and comes at a large computational

cost⁸⁵. The validation of the FF should take place at the level of periodic calculations, for

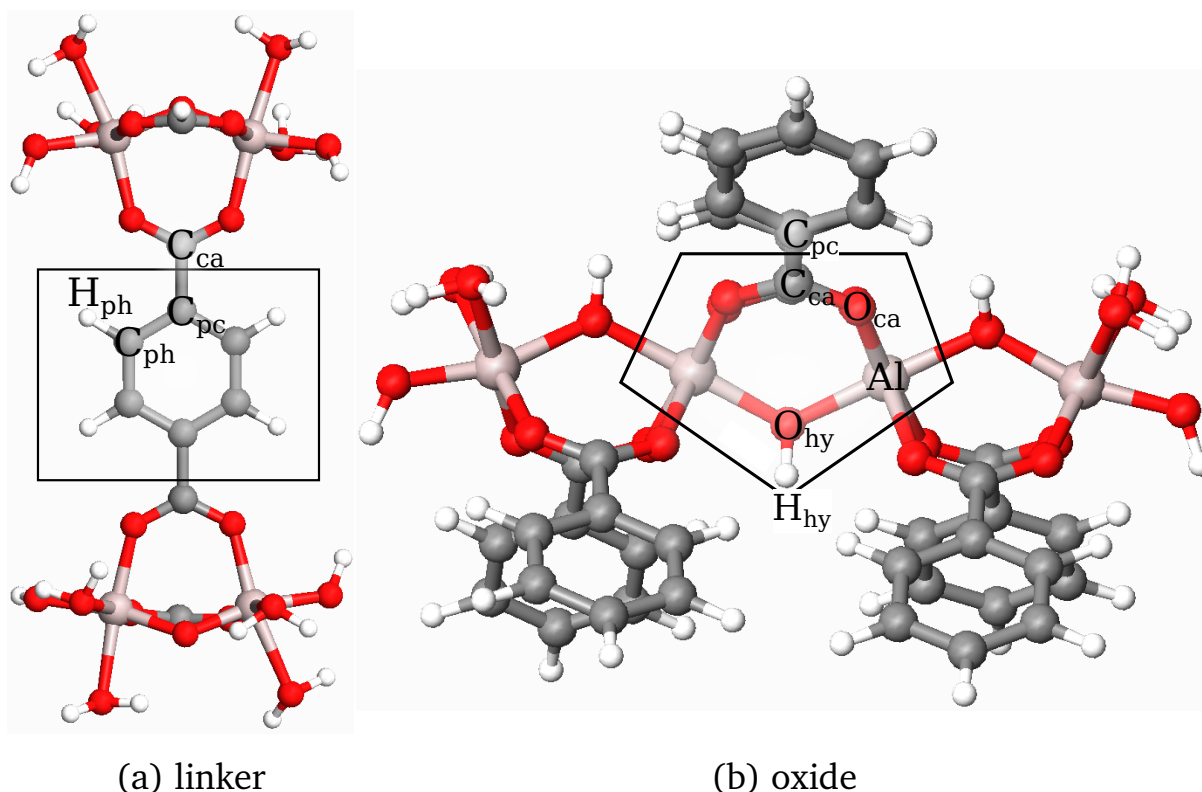


Figure 4: (left) Linker cluster and (right) oxide cluster on which QuickFF was performed. The solid line defines the core region used to define atom types relevant for the periodic system. Reprinted (adapted) with permission from ref. 18. Copyright (2014) American Chemical Society.

which the flexibility, the geometry, unit cell dimensions, energy profile of the breathing mode should be described appropriately.

Starting from an initial structure of the material, the atomic coordinates and unit cell parameters are fully relaxed during the geometry optimization of the periodic structure with the force field. The resulting equilibrium values of several bond lengths are compared with the ab initio predictions extracted from the extended cluster calculations as they are used as reference data in the parametrization of the FF (see Table 1). Both force fields (with and without out-of-plane terms) succeed in accurately reproducing the bond lengths (a more extended comparison including bending angles and dihedral angles is given in the Supporting Information). Furthermore, the table also reveals that the new QuickFF force field and the

ATYPES	Linker	Oxide	Previous	QuickFF	
				nooop	oop
AL-O _{CA}	1.93 ± 0.01	1.92 ± 0.01	1.93 ± 0.01	1.87 ± 0.00	1.86 ± 0.00
AL-O _{HY}	—	1.86 ± 0.00	1.88 ± 0.01	1.83 ± 0.00	1.82 ± 0.00
C _{CA} -C _{PC}	1.50 ± 0.00	1.49 ± 0.00	1.50 ± 0.00	1.49 ± 0.00	1.49 ± 0.00
C _{CA} -O _{CA}	1.27 ± 0.00	1.27 ± 0.00	1.27 ± 0.00	1.26 ± 0.00	1.26 ± 0.00
C _{PC} -C _{PH}	1.40 ± 0.00	1.41 ± 0.00	1.41 ± 0.00	1.40 ± 0.00	1.41 ± 0.00
C _{PH} -C _{PH}	1.39 ± 0.00	—	1.39 ± 0.00	1.39 ± 0.00	1.39 ± 0.00
C _{PH} -H _{PH}	1.08 ± 0.00	1.08 ± 0.00	1.08 ± 0.00	1.08 ± 0.00	1.08 ± 0.00
H _{HY} -O _{HY}	—	0.96 ± 0.00	0.91 ± 0.00	0.96 ± 0.00	0.96 ± 0.00

Table 1: Ab initio optimized bond lengths (in Å) of the linker and oxide cluster compared with the periodic predictions made by our previous¹⁸ force field and the present QuickFF force field. Two options are investigated in QuickFF: inclusion of out-of-plane distance terms (oop) or not (nooop).

previous force field perform equally.

The ultimate validation of the force field generated with QuickFF, is the prediction of a correct flexibility behavior for the unit cell. By starting from initial geometries close to the experimental structure of the narrow pore (np) and large pore (lp) phase, we can determine the unit cell dimensions for both phases with the force field. The definition of the unit cell dimensions is illustrated in the Supporting Information. In Table 2, we compare the various force-field predictions with the experimental results of Liu et al⁸⁶. We can conclude that all FF variants perform fairly well, however, the presence of an oop term in the valence potential energy improves the prediction of the large pore unit cell.

Finally, the energy profile along the interdiagonal angle θ is computed. This energy profile is characteristic for a breathing material, because the motion related to a variation in θ represents this breathing motion. The result is plotted in Figure 5. According to Walker et al.⁸⁷, the energy difference between np and lp should be in the range 33-42 kJ.mol⁻¹ depending on which functional is used in the DFT-D method. The force field, presented in our previous work¹⁸, predicts an energy difference of 60 kJ.mol⁻¹, which was outside the range

	Narrow pore				Large pore			
	Exp ^a	QuickFF		Prev ^b	Exp ^a	QuickFF		Prev ^b
		oop	nooop			oop	nooop	
a [Å]	20.82	19.32	19.22	19.57	16.91	16.66	16.05	17.05
b [Å]	6.61	6.75	6.73	6.53	6.62	6.71	6.73	6.59
c [Å]	6.87	6.10	6.10	6.25	12.67	12.77	13.59	12.91
α [deg]	90.00	89.98	95.26	87.89	90.00	89.98	90.00	90.00
β [deg]	90.00	90.20	90.41	89.43	90.00	90.01	90.00	90.00
γ [deg]	113.95	92.60	92.58	97.15	90.00	90.01	90.00	90.63
D [Å]	21.93	20.24	20.14	20.54	21.13	20.99	21.03	21.38
θ [deg]	36.52	35.04	35.15	35.41	73.68	74.95	80.49	74.25

Table 2: Comparison of the unit cell predicted by the force field with the experimental cell parameters (a) Ref. 86 (b) Ref. 18

suggested by Walker. At that point we argued that a scaling of the MM3-vdW parameters had a large impact on the quantitative energy differences between the large and narrow pore forms. The results generated by QuickFF in the two options (oop and nooop) demonstrate that the energy profile is very sensitive to the method of how dihedral forces are treated and the inclusion of out-of-plane motions. The QuickFF/nooop force field predicts an energy difference of about 39 kJ mol⁻¹ per unit cell, which is consistent with the range of Walker, while a slightly different parametrization due to incorporation of oop terms, increases the np-lp barrier to 49 kJ mol⁻¹, which more consistent with our previous force field. In our earlier force field (Ref. 18), the force constants corresponding to the Al-O_{CA}-C_{CA}-C_{PC} and Al-O_{CA}-C_{CA}-O_{CA} dihedrals had to be reparametrized to reproduce the periodic behavior more accurately. Therefore, an ab initio scan of the periodic structure along the interdiagonal angle θ was necessary at that point and thus the procedure required some manual interventions and additional generation of ab initio data. In this case, using QuickFF/oop, such manual interventions are no longer necessary and thus the procedure is more transparent to use to a broader set of MOFs. For MIL-53(Al), the prototype example of a flexible MOF, QuickFF successfully passed the validation and thus the protocol may be used to

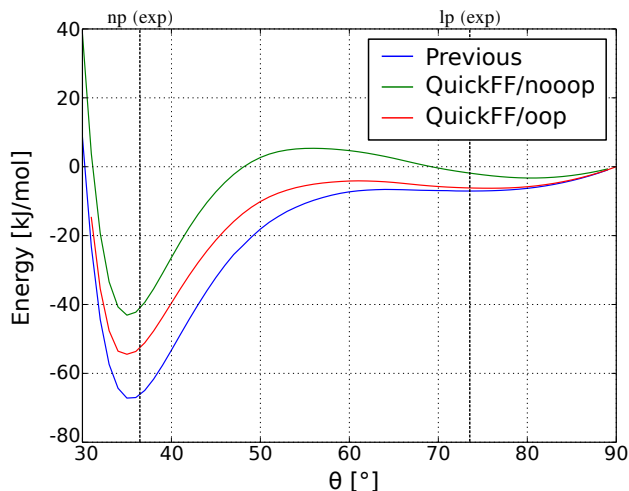


Figure 5: Breathing profile of Mil-53(Al) according to the new QuickFF force field (with the two options oop and nooop) and the previous force field (with unscaled MM3-vdW).

other hybrid flexible materials.

3.2.2 Validation for MOF-5: QuickFF versus MOF-FF

MOF-FF is the force field protocol developed by Schmid et al. and is very successful in generating force fields for a variety of hybrid materials, but as we mentioned before, manual interventions may prove necessary during the fitting procedure of the force field. For MOF-5 an assessment is made on the force field generated by QuickFF and by MOF-FF. Both methodologies have some common features but also some differences in the analytical FF expression for the description of the covalent part of the force field. In MOF-FF a Morse potential is used to describe the coordination bonds in which the metal is involved. Additionally, some stretch-stretch and stretch-bend cross terms are taken into account. We generated a force field using QuickFF starting from the same reference data of a single cluster (Figure 6), used for the MOF-FF force field⁵⁵. Instead of point charges the same spherical Gaussian charge distributions are employed in the two FF protocols.

A first validation of the force fields concerns the reproduction of the equilibrium geometry and the vibrational frequencies of the model system. Bond lengths are geometrical parame-

ters, that are the most sensitive to variations of the FF parameters. They are tabulated in Table 3. There is a slight preference for MOF-FF in reproducing the ab-initio reference data. The largest deviation is noticed in the metal-oxygen bond distance O_{ce} -Zn, which is slightly underestimated by QuickFF. The remaining geometrical parameters are all accurately reproduced; the whole list is reported in the SI. The final goal of the FF is its adequacy to predict

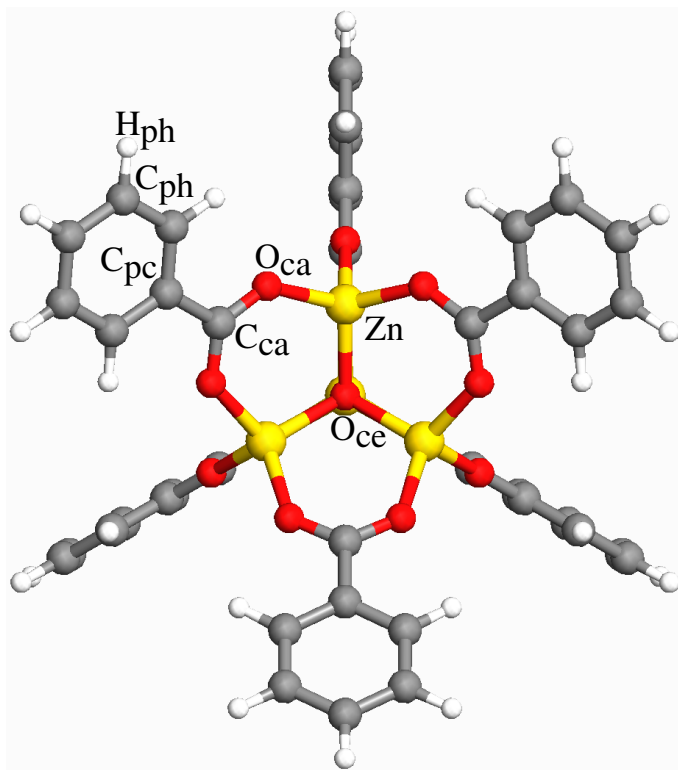


Figure 6: Structure of basic zinc benzoate as model system for MOF-5. All atomic types are given.

properties of the MOF-5 framework. Unit cell parameters are tabulated in Table 4, they were calculated by performing a full relaxation of the unit cell. Both force fields reasonably succeed in reproducing the experimental estimates, with a slight preference to MOF-FF. A serious test for the force fields is the prediction of the (low) frequencies of the normal modes. They are tabulated in the SI, but a one-to-one correspondence of the data, resulting from the two force fields, is not meaningful due to the degeneracies corresponding to each normal mode, which are obviously different for each FF (different terms). A correlation diagram is therefore more instructive and transparent (Figure 7). In this diagram, both the QuickFF

ATYPES	DFT	QuickFF	MOF-FF
C _{ca} -C _{pc}	1.497 ± 0.000	1.510 ± 0.000	1.497 ± 0.000
C _{ca} -O _{ca}	1.271 ± 0.000	1.274 ± 0.000	1.271 ± 0.000
C _{pc} -C _{ph}	1.404 ± 0.000	1.413 ± 0.000	1.402 ± 0.000
C _{ph} -C _{ph}	1.398 ± 0.002	1.402 ± 0.000	1.399 ± 0.001
C _{ph} -H _{ph}	1.090 ± 0.001	1.090 ± 0.001	1.093 ± 0.001
O _{ca} -Zn	1.960 ± 0.000	1.968 ± 0.000	1.962 ± 0.000
O _{ce} -Zn	1.963 ± 0.000	1.921 ± 0.000	1.967 ± 0.000

Table 3: Comparison of bond lengths in the benzoate cluster as predicted by DFT, QuickFF and MOF-FF.

and MOF-FF frequencies are sorted numerically and plotted against each other. The step-wise increase of the frequencies in the correlation diagram (best visualized in the inset of the figure) points toward a different degeneracy observed in the QuickFF frequencies, but the global trend of the two sets of data is similar at least for frequencies below 1400 cm⁻¹.

	QuickFF	MOF-FF	exp⁸³
<i>a</i> [Å]	26.173	26.080	25.885
<i>b</i> [Å]	26.173	26.080	25.885
<i>c</i> [Å]	26.173	26.080	25.885
α [deg]	90.000	90.000	90.000
β [deg]	90.000	90.000	90.000
γ [deg]	90.000	90.000	90.000

Table 4: Comparison of the unit cell of MOF-5 as predicted by QuickFF, MOF-FF and experiment.

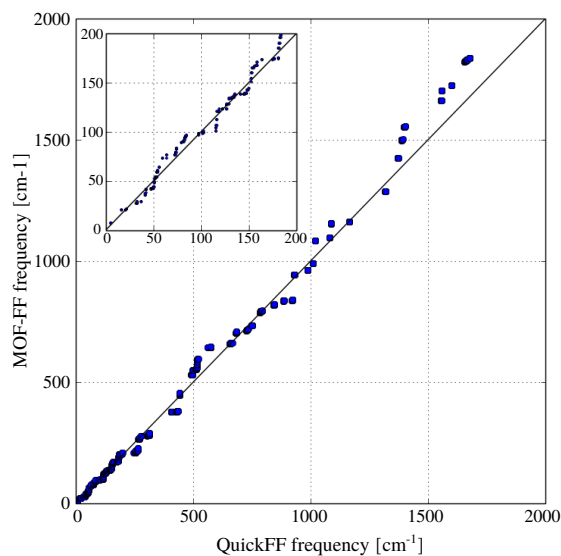


Figure 7: Comparison of frequencies of MOF-5 as calculated by QuickFF and MOF-FF.

4 Conclusions

Quick FF is a new and fast protocol to derive force fields for isolated and complex molecular systems from ab initio calculations. The development of the new software is inspired by the quest from the MOF community to determine in a fast, transparent and easy way force fields for these new type of hybrid materials. The input data for QuickFF consists of ab initio equilibrium geometries and a Hessian on smaller building units. The mathematical expression for the covalent energy terms is kept simple using harmonic terms for bond lengths, bending angles and out-of-plane distances and single cosine functions for dihedral angles. Such an approach was preferred to ensure robustness and to avoid fitting deficiencies as much as possible. The parameters of the electrostatic and van der Waals interactions are assumed to be known a priori and can be taken from population schemes that are available in literature. An option is built in to spread the atomic point charge over a spherical Gaussian distribution function centered on the nucleus. The resulting force fields are intended for direct use in molecular simulations. If they are too simple to describe more complex systems, they still provide a first generation force field for further fine tuning.

A new methodology was implemented that relies on the generation of perturbation tra-

jectories around the equilibrium. For each internal coordinate a trajectory was constructed to minimize the strain along the trajectory generated by the other IC's. Finally, all force constants were refined using a least-square cost function that measures the error between the force field and ab initio Hessian expressed in Cartesian coordinates. In QuickFF, there is no need for complicated cost functions nor for an introduction of weight factors.

The QuickFF procedure was illustrated by applying it on a large set of organic molecules, for which the new force fields succeeded in reproducing the ab initio geometry and Hessian in equilibrium. Furthermore QuickFF performed well in comparison with general force fields such as UFF and GAFF. Especially the introduction of a term containing out-of-plane distances was shown to be very valuable.

To show the validity of the protocol for generation of force fields on MOFs, two materials (MIL-53(Al) and MOF-5) were studied for which force fields are available in literature but which were constructed using several manual interventions. The force fields for the periodic structures are constructed on basis of a building block concept as originally introduced by Schmid and co-workers. Ab initio calculations are performed on smaller building units, from which force-field parameters are deduced using the QuickFF methodology. Afterward the parameters are merged in an appropriate way to generate a force field for the periodic structure. For MIL-53(Al), QuickFF fully complies with the expectations, the force field was able to reproduce the geometries, unit cell dimensions and relative stabilities of the large and narrow pore phases. Furthermore the new force field was able to predict a correct breathing profile for this flexible material.

In addition, QuickFF and MOF-FF were compared for generating a force field for MOF-5. The two FF methodologies succeed in achieving the expected accuracy. The more elaborated MOF-FF turned out to be slightly superior to the present version of QuickFF in reproducing properties of the framework. QuickFF was developed within the scope of offering a fast and easy recipe to the MOF community to construct a valuable FF for any MOF structure.

QuickFF has been implemented in a user-friendly Python code and is available via <http://github.com/molmod/QuickFF>. The program is clearly valuable for the screening of large databases of MOFs and for the derivation of their properties based on extensive molecular dynamics or Monte Carlo simulations.

Program Availability

The Python code can be downloaded from the web-interface to the revision control system Git: <http://github.com/molmod/QuickFF>.

Acknowledgments

This work is supported by the Fund for Scientific Research Flanders (FWO), the Research Board of Ghent University (BOF) and BELSPO in the frame of IAP/7/05. Funding was also received from the European Research Council under the European Community's Seventh Framework Programme [FP7(2007-2013) ERC grant agreement number 240483]. Computational resources (Stevin Supercomputer Infrastructure) and services were provided by Ghent University.

Supporting Information

Additional Supporting Information may be found in the online version of this article. The following additional information is included: more details and examples on the built-in function to choose atom types, a detailed description of the dihedral potential, details concerning the perturbation trajectories, a description of the procedure to select molecules for the training set and more details and results off the force fields of Mil-53(Al) and MOF-5.

References

1. Charifson P. *Practical Application of Computer-aided Drug Design*. Marcel Dekker: New York, 1997.
2. Leach A. *Molecular Modelling. Principles and Applications*. 2 edn., Prentice-Hall: Harlow, England, 2001.
3. Cramer C. *Essentials of Computational Chemistry: Theories and Models*. John Wiley & Sons: New York, 2002.
4. Kollman P, Case D. *In Burger's Medicinal Chemistry and Drug Discovery*, vol. 1: Drug Discovery. 6 edn., John Wiley & Sons: New York, 2003.
5. Düren T, Sarkisov L, Yaghi OM, Snurr RQ. Design of new materials for methane storage. *Langmuir* 2004; **20**:2683–2689.
6. Seminario J, Derosa P, Cordova L, Bozard B. A molecular device operating at terahertz frequencies: Theoretical simulations. *IEEE T. Nanotechnol.* 2004; **3**(1):215–218.
7. Kuang YD, Shi SQ, Chan PKL, Chen CY. A continuum model of the van der waals interface for determining the critical diameter of nanopumps and its application to analysis of the vibration and stability of nanopump systems. *Int. J. Nonlin. Sci. Num.* 2010; **11**(2):121–133.
8. Bushuev YG, Sastre G. Atomistic simulation of water intrusion/extrusion in itq-4 (ifr) and zsm-22 (ton): The role of silanol defects. *J. Phys. Chem. C* 2011; **115**:21 942–21 953.
9. Somers W, Bogaerts A, van Duin A, Huygh S, Bal K, Neyts E. Temperature influence on the reactivity of plasma species on a nickel catalyst surface: An atomic scale study. *Catal. Today* 2013; **211**:131–136.
10. Schyman P, Jorgensen WL. Exploring adsorption of water and ions on carbon surfaces using a polarizable force field. *J. Phys. Chem. Lett.* 2013; **4**:468–474.

11. Yang Q, Zhong C. Molecular simulation of adsorption and diffusion of hydrogen in metal-organic frameworks. *J. Phys. Chem. B* 2005; **109**:11 862–11 864.
12. Garberoglio G, Skoulidas A, Johnson J. Adsorption of gases in metal organic materials: Comparison of simulations and experiments. *J. Phys. Chem. B* 2005; **109**(27):13 094–13 103.
13. Salles F, Ghoufi A, Maurin G, Bell RG, Mellot-Draznieks C, Ferey G. Molecular dynamics simulations of breathing mofs: Structural transformations of mil-53(cr) upon thermal activation and co₂ adsorption. *Angew. Chem. Int. Ed.* 2008; **47**:8487.
14. Amirjalayer S, Tafipolsky M, Schmid R. Molecular dynamics simulation of benzene diffusion in mof-5: Importance of lattice dynamics. *Angew. Chem. Int. Ed.* 2007; **46**:463–466.
15. Wehring M, Gascon J, Dubbeldam D, Kapteijn F, Snurr RQ, Stallmach F. Self-diffusion studies in cubtc by pfg nmr and md simulations. *J. Phys. Chem. C* 2010; **114**(23):10 527–10 534.
16. Salles F, Jovic H, Devic T, Guillerm V, Serre C, Koza MM, Ferey G, Maurin G. Diffusion of binary co₂/ch₄ mixtures in the mil-47(v) and mil-53(cr) metalorganic framework type solids: A combination of neutron scattering measurements and molecular dynamics simulations. *J. Phys. Chem. C* 2013; **117**:11 275–11 284.
17. Liu B, Smit B. Comparative molecular simulation study of co₂/n₂ and ch₄/n₂ separation in zeolites and metal-organic frameworks. *Langmuir* 2009; **25**:5918–5926.
18. Vanduyfhuys L, Verstraelen T, Vandichel M, Waroquier M, Van Speybroeck V. Ab initio parametrized force field for the flexible metalorganic framework mil-53(al). *J. Chem. Theory Comput.* 2012; **8**(9):3217–3231.
19. Ghysels A, Vanduyfhuys L, Vandichel M, Waroquier M, Van Speybroeck V, Smit B. On the thermodynamics of framework breathing: A free energy model for gas adsorption in mil-53. *J. of Phys. Chem. C* 2013; **117**(22):11 540–11 554.

20. Rappé A, Casewit C, Colwell K, Goddard W, Skiff W. Uff, a full periodic table force field for molecular mechanics and molecular dynamics simulations. *J. Am. Chem. Soc.* 1992; **114**(25):10 024–10 035.
21. Wang J, Wolf R, Caldwell J, Kollman P, Case D. Development and testing of a general amber force field. *J. Comput. Chem.* 2004; **25**(9):1157–1174.
22. Mayo S, Olafson B, Goddard W. Dreiding: a generic force field for molecular simulations. *J. Phys. Chem.* 1990; **94**:8897.
23. Jorgensen W, Tirado-Rives J. The opls [optimized potentials for liquid simulations] potential functions for proteins, energy minimizations for crystals of cyclic peptides and crambin. *J. Am. Chem. Soc.* 1988; **110**:1657–1666.
24. Jorgensen WL, Maxwell DS, Tirado-Rives J. Development and testing of the opls all-atom force field on conformational energetics and properties of organic liquids. *J. Am. Chem. Soc.* 1996; **118**:11 225–11 236.
25. Weiner S, Kollman P, Nguyen D, Case D, Singh U, Ghio C, Alagona G, Jr SP, Weiner P. A new force field for molecular mechanical simulation of nucleic acids and proteins. *J. Am. Chem. Soc.* 1984; **106**:765–784.
26. Weiner S, Kollman P, Nguyen D, Case D. An all atom force field for simulations of proteins and nucleic acids. *J. Comput. Chem.* 1986; **7**:230–252.
27. Cornell W, Cieplak P, Bayly C, Gould I, Jr KM, Ferguson D, Spellmeyer D, Fox T, Caldwell J, Kollman P. A second generation force field for the simulation of proteins, nucleic acids, and organic molecules. *J. Am. Chem. Soc.* 1995; **117**:5179–5197.
28. MacKerell A, Bashford D, Bellott, Dunbrac, Evanseck JD, Field MJ, Fischer S, Gao J, Guo H, Ha S, *et al.*. All-atom empirical potential for molecular modeling and dynamics studies of proteins. *J. Phys. Chem. B* 1998; **102**:3586–3616.
29. MacKerell A, Banavali N, Foloppe N. Development and current status of the charmm force field for nucleic acids. *Biopolymers* 2001; **56**:257–265.

30. MacKerell A, Feig M, Brooks C. Extending the treatment of backbone energetics in protein force fields: limitations of gas-phase quantum mechanics in reproducing protein conformational distributions in molecular dynamics simulations. *J Comput Chem* 2004; **25**:1400–1415.
31. Allinger N, Yuh Y, Lii J. Molecular mechanics. the mm3 force field for hydrocarbon 3. 1. *J. Am. Chem. Soc.* 1989; **111**(23):8551–8566.
32. Allinger N, Chen K, Lii J. An improved force field mm4 for saturated hydrocarbons. *J. Comput. Chem.* 1996; **17**(5):642–668.
33. Cacelli I, Prampolini G. Parametrization and validation of intramolecular force fields derived from dft calculations. *J. Chem. Theory Comput.* 2007; **3**(5):1803–1817.
34. Barone V, Cacelli I, De Mitri N, Licari D, Monti S, Prampolini G. Joyce and ulysses: integrated and user-friendly tools for the parameterization of intramolecular force fields from quantum mechanical data. *Phys. Chem. Chem. Phys.* 2013; **15**:3736–3751.
35. Burger SK, Lacasse M, Verstraelen T, Drewry J, Gunning P, Ayers PW. Automated parametrization of amber force field terms from vibrational analysis with a focus on functionalizing dinuclear zinc(ii) scaffolds. *J. Chem. Theory Comput.* 2012; **8**:554–562.
36. Huang L, Roux B. Automated force field parameterization for nonpolarizable and polarizable atomic models based on ab initio target data. *J. Chem. Theory Comput.* 2013; [Dx.doi.org/10.1021/ct4003477](https://doi.org/10.1021/ct4003477).
37. Vanommeslaeghe K, Hatcher E, Acharya C, Kundu S, Zhong S, Shim J, Darian E, Guvench O, Lopes P, Vorobyov I, *et al.*. Charmm general force field: A force field for drug-like molecules compatible with the charmm all-atom additive biological force fields. *J. Comput. Chem.* 2010; **31**(4):671.
38. Mayne CG, Saam J, Schulten K, Tajkhorshid E, Gumbart JC. Rapid parameterization of small molecules using the force field toolkit. *J. Comput. Chem.* 2013; **34**:2757–2770, [doi:10.1002/jcc.23422](https://doi.org/10.1002/jcc.23422).

39. Grimme S. A general quantum mechanically derived force field (qmddf) for molecules and condensed phase simulations. *J. Chem. Theory Comput.* Jan 2014; **10**:4497–4514.
40. Grimme S, Antony J, Ehrlich S, Krieg H. A consistent and accurate ab initio parametrization of density functional dispersion correction (dft-d) for the 94 elements h-pu. *J. Chem. Phys.* 2010; **132**:154 104.
41. Wilmer C, Leaf M, Lee C, Farha O, Hauser B, Hupp J, Snurr RQ. Large-scale screening of hypothetical metalorganic frameworks. *Nat. Chem.* 2012; **4**:83.
42. Colon Y, Snurr R. High-throughput computational screening of metal-organic frameworks. *Chem. Soc. Rev.* 2014; **43**:5735–5749.
43. Salles F, Jobic H, Ghoufi A, Llewellyn PL, Serre C, Bourelly S, Serre C, Vincent D, Loera-Serna S, Filinchuk Y, *et al.*. Transport diffusivity of co2 in the highly flexible metal-organic framework mil-53(cr). *Angew. Chem. Int. Ed.* 2009; **48**:8335–8339.
44. Ramsahye NA, Maurin G, Bourelly S, Llewellyn PL, Serre C, Loiseau T, Devic T, Ferey G. Probing the Adsorption Sites for CO2 in Metal-Organic Frameworks Materials MIL-53(Al,Cr) and MIL-47(V) by Density Functional Theory. *J. Phys. Chem. C* 2008; **112**:514–520.
45. Karra JR, Walton KS. Molecular simulations and experimental studies of co2, co and n2 adsorption in metal-organic frameworks. *J. Phys. Chem. C* 2010; **114**:15 735–15 740.
46. Arstad B, Fjellvag H, Kongshaug KO, Swang O, Blom R. Amine functionalised metal organic frameworks (MOFs) as adsorbents for carbon dioxide. *Adsorption* 2008; **14**:755–762.
47. Stavitski E, Pidko E, Couck S, Remy T, Hensen EJ, Weckhuysen BM, Denayer J, Gascon J, Kapteijn F. Complexity behind CO2 Capture on NH2-MIL-53(Al). *Langmuir* 2011; **27**:3970–3976.
48. Llewellyn PL, Horcajada P, Maurin G, Devic T, Rosenbach N, Bourelly S, Serre C, Vincent D, Loera-Serna S, Filinchuk Y, *et al.*. Complex adsorption of short linear alkanes

- in the flexible metal-organic framework mil-53(fe). *J. Am. Chem. Soc.* 2009; **131**:13 002–13 008.
49. Pera-Titus M, Lescouet T, Aguado S, Farrusseng D. Quantitative characterization of breathing upon adsorption for series of amino-functionalized mil-53. *J. Phys. Chem. C* 2011; **116**:9507–9516.
 50. Coudert FX, Mellot-Draznieks C, Fuchs AH, Boutin A. Double structural transition in hybrid material mil-53 upon hydrocarbon adsorption: the thermodynamics behind the scenes. *J. Am. Chem. Soc.* 2009; **131**:3442–3443.
 51. Llewellyn PL, Maurin G, Devic T, Loera-Serna S, Rosenbach N, Serre C, Bourelly S, Horcajada P, Filinchuk Y, Ferey G. Prediction of the conditions for breathing of metal organic framework materials using a combination of x-ray powder diffraction, microcalorimetry, and molecular simulation. *J. Am. Chem. Soc.* 2008; **130**:12 808–12 814.
 52. Tafipolsky M, Amirjalayer S, Schmid R. Ab initio parametrized mm3 force field for the metal-organic framework mof-5. *J. Comput. Chem.* 2007; **28**:1169–1176.
 53. Tafipolsky M, Schmid R. Systematic First Principles Parameterization of Force Fields for Metal-Organic Frameworks using a Genetic Algorithm Approach. *J. Phys. Chem.* 2009; **113**:1341–1352.
 54. Tafipolsky M, Amirjalayer S, Schmid R. First-Principles-Derived Force Field for Copper Paddle-Wheel-Based Metal-Organic Frameworks. *J. Phys. Chem. C* SEP 2 2010; **114**(34):14 402–14 409.
 55. Bureekaew S, Amirjalayer S, Tafipolsky M, Spickermann C, Roy TK, Schmid R. Mof-ff - a flexible first-principles derived force field for metal-organic frameworks. *Phys. Status Solidi B* 2013; **250**:1128–1141.
 56. Bristow J, Tiana D, Walsh A. Transferable force field for metal-organic frameworks from first-principles: Btw-ff. *J. Chem. Theory Comput.* Jan 2014; **10**:4644–4652.
 57. Bader R. Atoms in molecules. *Acc. Chem. Res.* 1985; **18**:9–15.

58. Addicoat M, Vankova N, Akter I, Heine T. Extension of the universal force field to metal-organic frameworks. *J. Chem. Theory Comput.* 2014; **10**:880–891.
59. Frisch M, Trucks G, Schlegel H, Scuseria G, Robb M, Cheeseman J, Scalmani G, Barone V, Mennucci B, Petersson G, *et al.*; Gaussian 09 Revision A.02, Gaussian Inc. Wallingford CT 2009.
60. Maple J, Dinur U, Hagler A. Derivation of force fields for molecular mechanics and dynamics from ab initio energy surfaces. *Proc. Natl. Acad. Sci. USA* 1988; **85**:5350–5354.
61. Hirshfeld F. Bonded-atom fragments for describing molecular charge densities. *Theor. Chim. Acta* 1977; **44**:129.
62. Bultinck P, Van Alsenoy C, Ayers PW, Carbo-Dorca R. Critical analysis and extension of the hirshfeld atoms in molecules. *J. Chem. Phys.* 2007; **126**:144 111.
63. Verstraelen T, Ayers PW, Van Speybroeck V, Waroquier M. Hirshfeld-e partitioning: Aim charges with an improved trade-off between robustness and accurate electrostatics. *J. Chem. Theory Comput.* 2013; **9**(5):2221–2225.
64. Bayly C, Cieplak P, Cornell W, Kollman P. A well-behaved electrostatic potential based method using charge restraints for deriving atomic charges: the resp model. *J. Phys. Chem.* 1993; **97**:10 269–10 280.
65. Burger SK, Ayers PW, Schofield J. Efficient parameterization of torsional terms for force fields. *J. Comput. Chem.* 2014; **35**(19):1438–1445.
66. Kraft, D. A, Software package for sequential quadratic programming, 1988, Tech. Rep. DFVLR-FB 88-28, DLR German Aerospace Center - Institute for Flight Mechanics, Koln, Germany.
67. Bolton E., Wang Y., Thiessen P.A., Bryant S.H., PubChem: Integrated Platform of Small Molecules and Biological Activities. Chapter 12 IN Annual Reports in Computational Chemistry, Volume 4, American Chemical Society, Washington, DC, 2008 April.

68. O’Boyle N, Banck M, James C, Morley C, Vandermeersch T, Hutchison G. Open babel: An open chemical toolbox. *J. Cheminf.* 2011; **3**(1):33–14.
69. Becke A. Density-functional exchange-energy approximation with correct asymptotic behavior. *Phys. Rev. A* 1988; **38**:3098.
70. Becke A. Density-functional thermochemistry. iii. the role of exact exchange. *J. Chem. Phys.* 1993; **98**:5648–5652.
71. Lee C, Yang W, Parr R. Development of the colle-salvetti correlation-energy formula into a functional of the electron density. *Phys. Rev. B* 1988; **37**:785.
72. Zygmunt S, Mueller R, Curtiss L, Iton L. An assessment of density functional methods for studying molecular adsorption in cluster models of zeolites. *Theochem* 1998; **430**:9–16.
73. Sousa S, Fernandes P, Ramos M. General performance of density functionals. *J. Phys. Chem. A* 2007; **111**:10 439–10 452.
74. Krishnan R, Binkley JS, Seeger R, Pople JA. Self-consistent molecular orbital methods. xx. a basis set for correlated wavefunctions. *J. Chem. Phys.* 1980; **72**(1):650–654.
75. McLean AD, Chandler GS. Contracted gaussian basis sets for molecular calculations. i. second row atoms, z=1118. *J. Chem. Phys.* 1980; **72**(10):5639–5648.
76. Frisch MJ, Pople JA, Binkley JS. Self-consistent molecular orbital methods 25: Supplementary functions for gaussian basis sets. *J. Chem. Phys.* 1984; **80**:3265–3269.
77. T. Verstraelen, S. Vandenbrande, M. Chan, F. H. Zadeh, C. González, P. A. Limacher, A. Malek, Horton 1.2.1, <http://theochem.github.com/horton/>,2014.
78. T. Verstraelen, L. Vanduyfhuys, S. Vandenbrande, *Yaff, yet another force field*, <http://molmod.ugent.be/software/>.
79. Ghysels A, Verstraelen T, Hemelsoet K, Waroquier M, Van Speybroeck V. TAMkin: A versatile package for vibrational analysis and chemical kinetics. *J. Chem. Inf. Model.* Aug 2010; **50**(9):1736–1750.

80. Zhao Y, Truhlar D. The m06 suite of density functionals for main group thermochemistry, thermochemical kinetics, noncovalent interactions, excited states, and transition elements: two new functionals and systematic testing of four m06-class functionals and 12 other functionals. *Theor. Chem. Account* 2008; **120**:215–241.
81. Zhao Y, Truhlar D. Density functionals with broad applicability in chemistry. *Acc. Chem. Res.* 2008; **41**:157–167.
82. Loiseau T, Serre C, Huguenard C, Fink G, Taulelle F, Henry M, Bataille T, Férey G. A rationale for the large breathing of the porous aluminum terephthalate (mil-53) upon hydration. *Chem. Eur. J.* 2004; **10**:1373–1382.
83. Li H, Eddaoudi M, O’Keeffe M, Yaghi O. Design and synthesis of an exceptionally stable and highly porous metal-organic framework. *Nature* 1999; **402**:276.
84. Yot P, Boudene Z, Macia J, Granier D, Vanduyfhuys L, Verstraelen T, Speybroeck VV, Devic T, Serre C, Férey G, *et al.*. Metal-organic frameworks as potential shock absorbers: the case of the highly flexible mil-53(al). *Chem Commun (Camb)* Aug 2014; **50**:9462–9464.
85. Piccini G, Sauer J. Quantum chemical free energies: Structure optimization and vibrational frequencies in normal modes. *Journal of Chemical Theory and Computation* 2013; **9**(11):5038–5045, doi:10.1021/ct4005504.
86. Liu Y, Her J, Dailly A, Ramirez-Cuesta A, Neumann D, Brown C. Reversible structural transition in mil-53 with large temperature hysteresis. *J. Am. Chem. Soc.* 2008; **130**:11 813–11 818.
87. Walker A, Civalleri B, Slater B, Mellot-Draznieks C, Corà F, Zicovich-Wilson C, Román-Pérez G, Soler J, Gale J. Flexibility in a metalorganic framework material controlled by weak dispersion forces: The bistability of mil-53(al). *Angew. Chem. Int. Ed.* 2010; **49**:7501–7503.